PDMS Flow Sensors With Graphene Piezoresistors Using 3D Printing and Soft Lithography

Kamat, Amar M; Jayawardhana, Bayu; Kottapalli, Ajay Giri Prakash

Published in:
2020 IEEE SENSORS Proceedings

DOI:
10.1109/SENSORS47125.2020.9278740

PDMS Flow Sensors With Graphene Piezoresistors Using 3D-Printing and Soft Lithography

Amar M. Kamat[1,*], Bayu Jayawardhana[2], *Senior Member, IEEE*, Ajay G.P. Kottapalli[1,3]

[1]Advanced Production Engineering (APE) Group, University of Groningen, Groningen, the Netherlands

[2]Discrete Technology & Production Automation (DTPA) Group, University of Groningen, Groningen, the Netherlands

[3]MIT Sea Grant College Program, Massachusetts Institute of Technology (MIT), Cambridge, United States

[*]Corresponding author: a.m.kamat@rug.nl

***Abstract*—This paper reports the fabrication and characterization of a flexible piezoresistive flow sensor comprising a polydimethylsiloxane (PDMS) cantilever with a serpentine graphene nanoplatelets (GNP) strain gauge embedded at the cantilever base. A facile and cleanroom-free processing work flow involving a combination of high-resolution powder bed fusion and soft lithography was used to fabricate PDMS cantilevers (aspect ratio 20) with 150 µm × 150 µm microchannels on its surface. A high gauge factor of 55 (up to 5 times higher than reported in comparable piezoresistive flow sensors) was achieved using drop-casted GNP ink as the piezoresistive sensing element in the aforementioned microchannels. Finally, the use of the PDMS-graphene cantilever as an airflow sensor with enhanced sensitivity (20 times more than comparable piezoresistive cantilever sensors), low hysteresis, good repeatability, and bidirectional sensing capability was demonstrated.**

Keywords—flow sensor; graphene nanoplatelets; PDMS; gauge factor; piezoresistivity; 3D printing; cantilever

I. Introduction

Flow sensing finds applications in many industries and can be achieved using a variety of sensing principles including Bernoulli's principle (e.g. pitot tube), thermal transport (e.g. thermal anemometry), ultrasonic waves, electromagnetic induction, and drag force measurement. Cantilevers represent a simple and popular sensor design that is inspired by the high-aspect ratio flow sensors found in fish neuromasts [1], insect wind receptors [2], seal whiskers [3], and so on; here, the drag force applied by the fluid on the high-aspect ratio structure causes it to bend, and the extent of bending is calibrated against the fluid velocity [4]. Traditionally, piezoresistive cantilever flow sensors have been fabricated using standard microelectromechanical systems (MEMS) cleanroom processes involving surface or bulk micromachining techniques [5]–[7] which are often tedious, expensive, and limited in the choice of materials for both the piezoresistive sensing elements and the cantilever. Recent advances in flexible electronics [8] have enabled the incorporation of novel piezoresistive materials such as graphite ink [9], graphene-PDMS composites [10], conductive poly(3,4-ethylenedioxythiophene) polystyrene sulfonate (PEDOT/PSS) inks [11] etc. on flexible cantilevers, allowing larger bending strains and hence greater sensitivities to stimuli. Flexible cantilever flow sensors have been fabricated using Elastosil® (a conductive piezoresistive composite) [12] and laser-induced graphene (LIG) [13] as the piezoresistive strain gauge materials; however, the gauge factors reported were in the low range of 7 [12] to 11 [13]. In this paper, we demonstrate a facile method of fabricating a PDMS cantilever airflow sensor featuring a serpentine graphene nanoplatelets (GNP) strain gauge using high-resolution 3D printing, soft lithography, and drop-casting. The piezoresistive airflow sensors exhibited a high gauge factor, bidirectional sensing capability, excellent sensitivity, and repeatability over multiple cycles of operation.

II. Experimental details

A. Sensor fabrication

Powder bed fusion (SLM 125HL), a laser-based metal 3D printing technique, was used to fabricate a stainless steel master mold for the sensor structure. The 3D printer was equipped with a fiber laser (1 µm wavelength, 70 µm spot diameter) which was used to selectively melt and fuse 17-4 PH stainless steel powder particles (10–45 µm size distribution, 30 µm layer thickness) at a laser power of 200 W and a scanning speed of 800 mm/s. The mold comprised a negative imprint of the cantilever with predesigned serpentine protrusions near the fixed end, and was printed such that the cantilever length was perpendicular to the printing direction which allowed us to print minimum feature sizes of 140 µm in the build plane. PDMS solution (Sylgard™ 184, 10:1 monomer-to-curing agent ratio by weight) was poured into the mold, degassed, cured (125 °C for 20 minutes), and finally demolded to obtain cantilevers (20 mm × 3 mm × 1 mm, aspect ratio = 20) with serpentine microchannel imprints (150 µm × 150 µm, 6 turns, 12 mm total length) near the fixed end. Commercially obtained conductive GNP dispersion ink (Graphene Supermarket, 23 wt.% graphene, nanoplatelet thickness ~7 nm) was diluted with ethanol (1:4 by volume) and drop-casted into the serpentine microchannel where it flowed readily due to the capillary effect. The structure was subsequently annealed (100 °C for 1 hour) to form a GNP strain gauge which showed a baseline resistance of ~70 kΩ. Prior to testing, the sensor anchor was mounted at the end of a glass slide and the GNP contact pads were connected to copper tapes electrodes) using conductive silver epoxy (EPOTEK H20E). The fabrication process flow is illustrated in Fig. 1. A similar procedure was used to prepare uniaxial PDMS tensile samples (50 mm × 10 mm × 10 mm) with a GNP-filled surface microchannel (23 mm × 300 µm × 300 µm) for the GF measurement (Fig. 2a, inset).

This work was labeled by ITEA and funded by local authorities under the grant agreement ITEA-2018-17030-Daytime.

978-1-7281-6801-2/20/$31.00 ©2020 IEEE

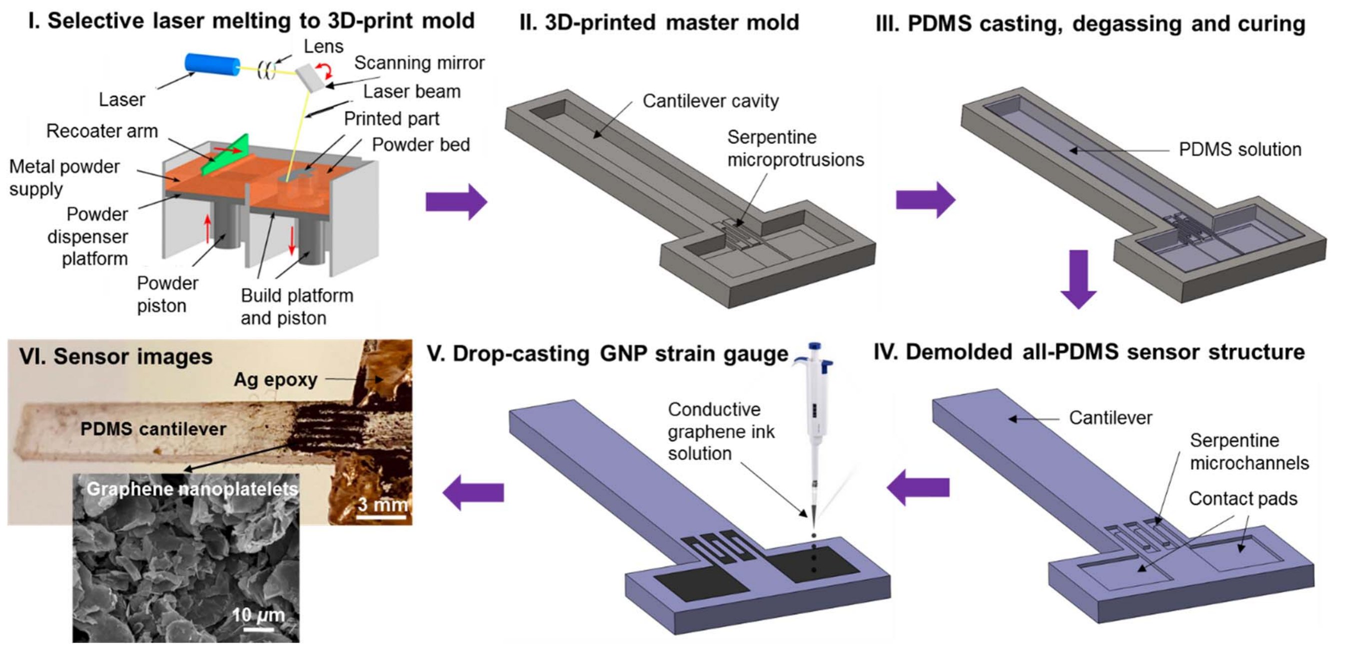

Figure 1. Fabrication of cantilever flow sensor using selective laser melting to 3D-print master mold, PDMS casting to obtain cantilever sensor structure, and GNP drop-casting into microchannels (150 µm × 150 µm) to form strain gauge (I to V); sensor photograph with 5000× SE micrograph of GNP (VI).

B. Sensor testing

The GF of the GNP strain gauge was measured by straining the tensile sample in a micromechanical testing machine (Kammrath and Weiss GmBH) in steps of 0.33 % strain (30 s hold per strain) while continuously recording its resistance using a digital multimeter (Keysight U2741A) at a sampling rate of 2 Hz (Keysight Benchvue software). The cantilever flow sensor was tested in a custom-built wind tunnel (test section 8 cm × 8 cm) where the airflow was generated using a variable-speed CPU cooling fan. The wind tunnel was calibrated using a commercial flow anemometer (Airflow Meter PCE-423) before the actual sensor tests. The cantilever sensor (secured at the end of a glass slide) was placed horizontally in the wind tunnel and the copper electrodes (outside the wind tunnel) were connected to a Wheatstone bridge circuit powered by a 9V battery. The voltage drop across the bridge was acquired using the NI-DAQ USB-6003 system and recorded on the NI Signal Express software at a sampling rate of 2 Hz. Each datum point plotted in Figs. 2–4 (at a given strain for the GF tensile sample in Fig. 2 and at a given airflow velocity for the airflow sensor in Figs. 3–4) represents the mean resistance measured over a period of at least 30 seconds at the respective strain/airflow velocity and averaged over five such independent tests to generate statistically significant data.

III. Results and Discussion

A. Gauge factor (GF) of GNP-on-PDMS

The average GF (Fig. 2) was calculated as the slope of the fractional resistance change ($\Delta R/R_0$) vs strain (ε) plot and was found to be 52 for loading and 56 for unloading (Fig. 2), higher than previously reported piezoresistive cantilever flow sensors (~ 7–11) [12,13], conventional metal strain gauges (~ 3) [14], or single layer graphene-on-PDMS strain gauges (~ 42) [15]. The high piezoresistive GF of GNP stems from the ability of the nanoplatelets to overcome weak van der Waal forces and easily slide over each other in tension and compression, thus changing the contact area and consequently the contact resistance [16]. Interestingly, the GF reported here is higher than the one reported by us (37) previously [17]. This can be attributed to two reasons: a) the testing methodology is different here ('quasi-static' where the resistance change at a given strain is calculated by holding the sample at that strain for 30 seconds) than in [17] ('dynamic' where the sample was strained continuously and the GF was calculated from the slope of the resistance change vs strain curve); and, b) the GF sample was only subjected to tension here while it was subjected to both tension and compression in [17]. The possible difference in GF of GNP in tension and compression is interesting and merits future studies.

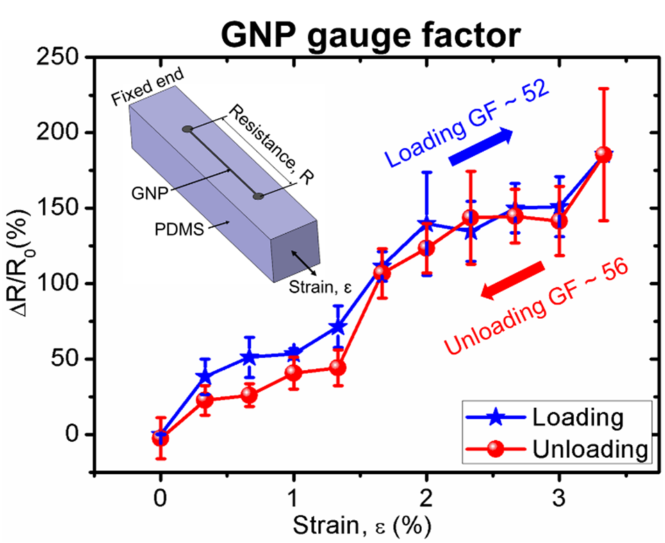

Figure 2. Gauge factor calculation of GNP-on-PDMS using tensile test

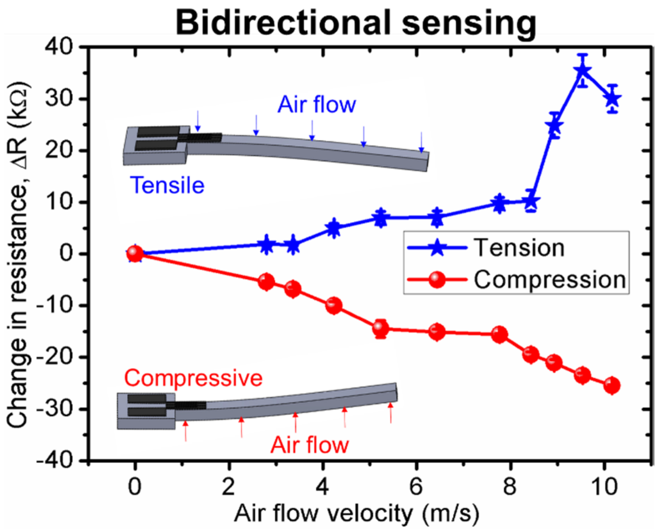

Figure 3. Bidirectional airflow sensing performance.

B. Cantilever flow sensor

The flow sensor was subjected to different airflow speeds in the wind tunnel in two configurations: airflow impinging upon the strain gauge face of the cantilever, and airflow impinging upon the opposite face. The former produced tensile strains while the latter produced compressive strains in the GNP strain gauge, causing a positive and negative resistance change, respectively (Fig. 3), demonstrating the bidirectional sensing of the sensor. Although the average resistance change for tensile strains was higher than for compressive strains, the sensor output was found to be have larger variance in the tensile state when compared to the compressive state, suggesting that the GNP strain gauge was more stable in the compressive state. Subsequent tests (Figs. 4 and 5) were thus performed only in the compressive configuration.

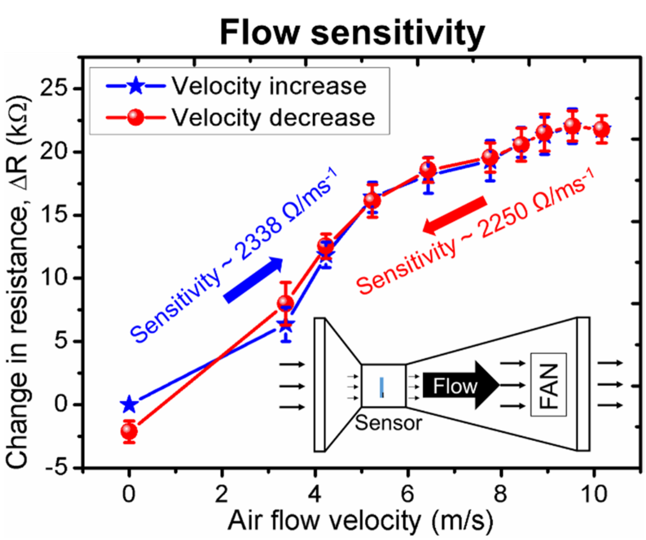

Figure 4. Hysteresis and sensitivity to airflow in wind tunnel.

The hysteresis of the sensor was tested by loading it sequentially with increasing airflow velocities (hold of 30 s per velocity) up to 10 m/s in the wind tunnel and then unloading it in the reverse sequence. As evident in Fig. 4, the sensor showed minimal hysteresis. However, the signal saturated at around 9 m/s of airflow velocity. The sensitivity of the piezoresistive airflow sensor (Fig. 4) was calculated using linear regression to be ~2300 Ω/ms^{-1}, which was more than 20 times higher than that reported recently by Kaidarova *et al.* [13] who used a laser-induced graphene (LIG) strain gauge on a flexible Kapton® cantilever flow sensor of comparable dimensions. It must also be noted that Kaidarova *et al.* [13] reported the sensitivity of their flow sensor for water flow which is always greater than the sensitivity to airflow, since the drag force exerted by a fluid on the cantilever is proportional to the density of the fluid, and water is around 800 times denser than air.

Finally, the repeatability of the sensor was tested at an airflow speed of 7.7 m/s. The airflow was switched on and off 20 times (30 s hold in each state) and the sensor resistance was recorded. It can be seen from Fig. 5 that the sensor displayed excellent repeatability, showing a variance of only 3 % around an average resistance change (ΔR) of 23 kΩ.

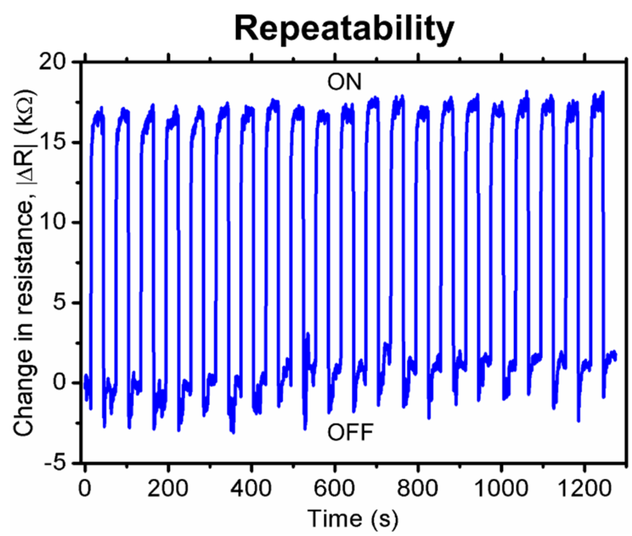

Figure 5. Repeatability over 20 ON-OFF cycles at 7.7 m/s airflow speed.

IV. Conclusions

A cleanroom-free processing workflow comprising high-resolution 3D printing of a metallic mold, soft lithography to obtain a PDMS cantilever structure, and drop-casting of graphene nanoplatelet dispersion to form a piezoresistive strain gauge (150 μm × 150 μm cross section), was used to fabricate flexible airflow sensors. The sensing materials (graphene nanoplatelets on PDMS) displayed a high gauge factor of 55 in a uniaxial tensile test. The airflow sensors showed low hysteresis, excellent sensitivity and repeatability, bidirectional sensing capability, and in general compared favorably to cantilever flow sensors of similar sizes reported in the literature. Future work will focus on optimizing the fabrication process, improving sensor-to-sensor reproducibility, sealing the GNP strain gauge with PDMS to make the sensors waterproof, and using the sensors in wind flow measurement applications. Recent advances in high-resolution metal 3D printing (e.g. 'micro laser sintering' [18]) allow further miniaturization and can enable our methodology to fabricate flexible MEMS sensors with feature sizes as small as 15–30 μm.

References

[1] A. G. P. Kottapalli and M. Asadnia, “Lateral-Line Inspired MEMS Neuromast Sensors BT - Biomimetic Microsensors Inspired by Marine Life,” A. G. P. Kottapalli, M. Asadnia, J. Miao, and M. S. Triantafyllou, Eds. Cham: Springer International Publishing, 2017, pp. 1–21.

[2] M. Dijkstra, J. J. van Baar, R. J. Wiegerink, T. S. J. Lammerink, J. H. de Boer, and G. J. M. Krijnen, “Artificial sensory hairs based on the flow sensitive receptor hairs of crickets,” *J. Micromechanics Microengineering*, vol. 15, no. 7, pp. S132–S138, 2005.

[3] G. Dehnhardt, B. Mauck, and H. Bleckmann, “Seal whiskers detect water movements,” *Nature*, vol. 394, no. 6690, pp. 235–236, 1998.

[4] J. Fraden, “Flow Sensors - Handbook of Modern Sensors: Physics, Designs, and Applications,” J. Fraden, Ed. New York, NY: Springer New York, 2010, pp. 399–429.

[5] Y. H. Wang, C. Y. Lee, and C. M. Chiang, “A MEMS-based air flow sensor with a free-standing microcantilever structure,” *Sensors*, vol. 7, no. 10, pp. 2389–2401, 2007.

[6] R. H. Ma, D. A. Wang, T. H. Hsueh, and C. Y. Lee, “A MEMS-based flow rate and flow direction sensing platform with integrated temperature compensation scheme,” *Sensors*, vol. 9, no. 7, pp. 5460–5476, 2009.

[7] Q. Zhang, W. Ruan, H. Wang, Y. Zhou, Z. Wang, and L. Liu, “A self-bended piezoresistive microcantilever flow sensor for low flow rate measurement,” *Sensors Actuators, A Phys.*, vol. 158, no. 2, pp. 273–279, 2010.

[8] M. Zou, Y. Ma, X. Yuan, Y. Hu, J. Liu, and Z. Jin, “Flexible devices: From materials, architectures to applications,” *J. Semicond.*, vol. 39, no. 1, 2018.

[9] X. Liu, M. Mwangi, X. Li, M. O’Brien, and G. M. Whitesides, “Paper-based piezoresistive MEMS sensors,” *Lab Chip*, vol. 11, no. 13, pp. 2189–2196, 2011.

[10] Y. S. Choi, M. J. Gwak, and D. W. Lee, “Polymeric cantilever integrated with PDMS/graphene composite strain sensor,” *Rev. Sci. Instrum.*, vol. 87, no. 10, 2016.

[11] M. Liu, Y. Zhao, Y. Shao, Q. Zhang, and C. Liu, “3D Printed Force Sensor with Inkjet Printed Piezoresistive Based Strain Gauge,” *Proc. IEEE Sensors*, vol. 2018-Octob, pp. 2018–2021, 2018.

[12] A. R. Aiyar, C. Song, S. H. Kim, and M. G. Allen, “An all-polymer airflow sensor using a piezoresistive composite elastomer,” *Smart Mater. Struct.*, vol. 18, no. 11, 2009.

[13] A. Kaidarova *et al.*, “Wearable multifunctional printed graphene sensors,” *npj Flex. Electron.*, vol. 3, no. 1, pp. 1–10, 2019.

[14] N. Lu, X. Wang, Z. Suo, and J. Vlassak, “Metal films on polymer substrates stretched beyond 50%,” *Appl. Phys. Lett.*, vol. 91, no. 22, pp. 1–4, 2007.

[15] S. Chun, Y. Choi, and W. Park, “All-graphene strain sensor on soft substrate,” *Carbon N. Y.*, vol. 116, pp. 753–759, 2017.

[16] M. Hempel, D. Nezich, J. Kong, and M. Hofmann, “A novel class of strain gauges based on layered percolative films of 2D materials,” *Nano Lett.*, vol. 12, no. 11, pp. 5714–5718, 2012.

[17] A. M. Kamat, Y. Pei, and A. G. P. Kottapalli, “Bioinspired Cilia Sensors with Graphene Sensing Elements Fabricated Using 3D Printing and Casting,” *Nanomaterials*, vol. 9, no. 7, p. 954, 2019.

[18] B. Nagarajan, Z. Hu, X. Song, W. Zhai, and J. Wei, “Development of Micro Selective Laser Melting: The State of the Art and Future Perspectives,” *Engineering*, vol. 5, no. 4, pp. 702–720, 2019.